Mechanical response evaluation of microcapsules from different slurries

Jessica Giro-Paloma[1], Camila Barreneche[1,2], Mònica Martínez[1]; Boštjan Šumiga[3], Ana Inés Fernández[1], Luisa F. Cabeza[2]

[1] Universitat de Barcelona. Faculty of Chemistry. Department of Materials Science and Metallurgical Engineering. C/ Martí i Franquès, 1, 08028 Barcelona (Spain). Phone: 34-934021298, Fax: 34-934035438, e-mail: jessicagiro@ub.edu, c.barreneche@ub.edu, monicamartinez@ub.edu, ana_inesfernandez@ub.edu

[2] GREA Innovació Concurrent. Edifici CREA. Universitat de Lleida. C/ Pere de Cabrera s/n, 25001-Lleida (Spain), Phone: 34-973003576, Fax: 34-973003575, e-mail: lcabeza@diei.udl.cat

[3] Iskra Mehanizmi d.o.o., Fužine 9, 1240 Kamnik. Phone: +38618309850, Fax:+38618309867, email: bostjan.sumiga@iskra-mehanizmi.si

Abstract

Thermal energy storage (TES) is one method to accumulate thermal energy. In TES, latent heat storage using phase change materials (PCM) has attracted a lot of interest, recently. Phase change slurries (PCS) consist on a carrier fluid binary system composed of water as the continuous phase and microencapsulated PCM as the dispersed phase. In this paper, two PCS to be used for TES in buildings were studied: Micronal® DS 5007 X, from BASF company, and PCS28, a laboratory made sample. Both samples were characterized using particle size distribution and scanning electron microscopy, to observe the regular spherical microcapsules, the surface morphology, and the wall shell thickness of the microcapsules. Atomic force microscopy was used to analyze the force needed to break the PCS microcapsules, a critical parameter when the PCS are to be used in active pumpable systems, and also to evaluate the effective Young's modulus. Both samples were studied with the microcapsules broken and unbroken. The physicochemical and thermal properties were reported in a previous paper, and it can be concluded that both are proper candidates to be used in TES building heating and cooling applications, but the acrylic shell microcapsules present better breakage resistance to be used in active systems.

Keywords: Phase Change Slurry (PCS); Particle Size Distribution (PSD); Scanning Electron Microscopy (SEM); Atomic Force Microscope (AFM); Mechanical characterization.

1. Introduction

Phase Change Materials (PCM) are well known in Thermal Energy Storage (TES) because of their capacity to absorb and slowly release the latent heat involved in the phase change process [1], as well as the ability to store a large amount of energy in relatively small volumes. TES with PCM achieves energy conservation in buildings with thermal comfort [2]. Energy storage is very important where the energy source is intermittent, as in solar energy field, and it can decrease the time between energy supply and energy demand. For this reason, energy storage is essential in energy conservation issues. There are some reported methods to include PCM in building walls [3] such as with impregnation. There is also in the literature some studies [4,5] exposing the introduction of PCM in constructive materials [6], such as gypsum [7,8], concrete [9], wood [10], etc. As there is leakage when mixing PCM with building materials, PCM has to be encapsulated for technical use and microcapsules were considered to address this issue [11]. Microencapsulated Phase Change Materials (MPCM) [12,13,14] are small vessels with a hydrophobic core material and a hard covering that accepts size alterations, maintains its shape and avoids corrosion problems. MPCM temperature remains unchanged during the heat absorption/release process and these can be applied in passive storage systems such as component in buildings envelopes [15], as well as, in sandwich panels [16]. MPCM can also be added to a fluid in order to be transported or pumped in an active storage system. They can be used in active storage systems such as pumping slurries [17,18,19], which are microcapsules suspensions or emulsions [20,21,22] using a dispersant agent in order to stabilize the distribution of the microcapsules in order to enhance its thermal behaviour. These slurries are known as Phase Change Slurries (PCS).

Different core/shell combinations that have been studied take into account the external polymer and the PCM nature (inorganic or organic) [23,24]. In this particular

case, the core samples are saturated hydrocarbon paraffin wax as the PCM. In this paper, two samples were characterized: Micronal® DS 5007 X provided by BASF® and a laboratory prepared suspension of microcapsules based on analysis and experimental optimization of in situ polymerisation technology for its preparation from scientific and patent literature [25]. This comparison aspect between both types of MPCM is very important as it is wanted to identify the best MPCM laboratory manufactured, or at least, the most similar commercial MPCM in a laboratory preparation. The two samples have melting temperatures around 24 - 28 ºC that are considered close to the indoor comfort temperature in buildings [26]. The physicochemical and thermal properties were evaluated in a previous paper [27].

The main objective of this study is to compare the physical and mechanical behaviour of two PCS samples able to be used in active systems in order to discern the most proper microcapsules for using them in a TES media for heating and cooling applications.

2. Materials and methods

2.1. Materials

Two types of PCS were studied in this paper. Micronal® DS 5007 X which has an acrylate polymer as a shell in a slurry medium, with a proportion of 2:5, (slurry + dispersant):water, and paraffin wax in the core. The other sample is PCS28 which is a laboratory made sample, and the shell was prepared with a melamine-formaldehyde (MF) resin. The paraffin wax inside the microcapsules PCS28 is *n*-octadecane. The phase change temperature of PCS28 is around 28 ºC and the proportional relation is 1:2, (slurry + dispersant):water [27]. The main reason for choosing these two types of MPCM was to compare the different mechanical behaviour related to the MPCM polymeric shell (acrylic or MF) and to decide which shell is better to microencapsulate the PCM.

2.2. Methodology

The size of the microcapsules was studied analysing the Particle Size Distribution (PSD). Also, by using Scanning Electron Microscopy (SEM) the dimensions of the

microcapsules can be measured. Finally, they were analyzed by Atomic Force Microscopy (AFM) [12,28,29], which is commonly used to examine the nano- or microscale properties of the surface and in close proximity surface regions. AFM is a powerful tool for evaluating polymeric materials on a sub-micrometer scale because it admits lesser forces and higher upper resolutions than nanoindenters [30]. In this study, it was identified the maximum force that can be applied on the top of microcapsules (dried PCS) to break them, analyzing the typical deflection-indentation curves. Besides, it was calculated the Effective Young's modulus (*E*) distribution in a specific region of each microsphere for the two studied samples. The tests were done at 23 ºC and 45 ºC for both samples, which is with the core material in solid and liquid phase.

2.2.1. Particle Size Measurements and Scanning Electron Microscopy

The Particle Size Distribution (PSD) was analyzed using a Beckman Coulter® LSTM 13 320 with Universal Liquid Module. The results were analyzed applying the Mie mathematical model, because it fits well for homogenous, spherical, and transparent or opaque particles with diameter below 50 μm. Afterwards, each sample was circulated separately a total of 10 minutes in order to estimate sample volume changes, to evaluate possible MPCM degradation or MPCM accumulation.

Samples morphologies were observed by Scanning Electron Microscopy (SEM) using a Jeol JSM-6510 instrument under vacuum atmosphere, high voltage (15 kV), and images obtained by secondary electrons. Furthermore, the microcapsules were broken in purpose applying a compressive strength to study the wall shell thickness, which is directly related with the mechanical properties of the microcapsules.

2.2.2. Atomic Force Microscopy (AFM)

The AFM equipment used to evaluate the mechanical properties of microcapsules (two dried PCS samples) was Multimode 8 and Nanoscope V electronics from Bruker with a Peak Force Quantitative Nanomechanics mode (QNM). The diamond probe used was from Bruker, with a 388 $nN \cdot nm^{-1}$ spring constant. Therefore, the peak force amplitude was 300 nm, the peak force frequency was 0.5 kHz, and finally, the maximum vertical force was 500 nN. One aliquot of each PCS was diluted in water in a small beaker. Then, 50 μl of this solution were poured on a freshly cleaved mica surface

under a N_2 stream until complete dryness. The samples were observed and mechanically tested without further treatment.

The goal of the first assay is to quantify the highest vertical force that the samples were able to resist after creating a permanent elastic deformation executing a force. It was obtained microcapsules images at 23ºC, and after that, it was applied a force on the top of the microcapsule until breaking the shell to perform a force curve. Subsequently, the particle was imaged again. This process was repeated three times at 23 ºC for each microcapsule (PCM in solid state); following that, PCS microcapsules temperature was raised to 45 ºC (PCM in liquid state), and the whole process was repeated again three times for each sample. A total of 18 tests were performed. The second set of experiments consists on testing the stiffness and calculate the Effective Young's modulus (*E*) of the dried PCS microcapsules at the two different temperatures performing two repetitions at 23 ºC and 45 ºC (PCM in solid and liquid state, respectively). In all the cases, the temperature was measured with a micro-thermocouple type-K in contact with the sample holder.

3. Results and discussion

3.1. Particle Size Measurements

3.1.1. Particle Size Distribution (PSD)

PSD was evaluated following the Mie mathematic model, and Table 1 lists the main results obtained. The parameter d_{10} means that 10 % of the volume of the particles had a diameter below the given value; for d_{50}, 50 % of the particles had a diameter below the given value, and finally, 90 % of particles had a size volume below d_{90}.

Table 1. Particle Size Distribution results from microcapsules under study

	Micronal® DS 5007 X	PCS28
PSD d_{10} (μm)	2.79	0.14
PSD d_{50} (μm)	4.88	3.46
PSD d_{90} (μm)	7.48	6.62

PSD mean (μm)	4.88	3.14
Standard deviation (μm)	2.09	2.62

At the light of the results, PCS28 presents lower values than Micronal® DS 5007X. Thereby, the repeatability over the measurements is shown in Figure 1 for Micronal® DS 5007 X. The profile curves obtained are almost identical, showing a quite narrow distribution, being assured the repeatability between the different experiments.

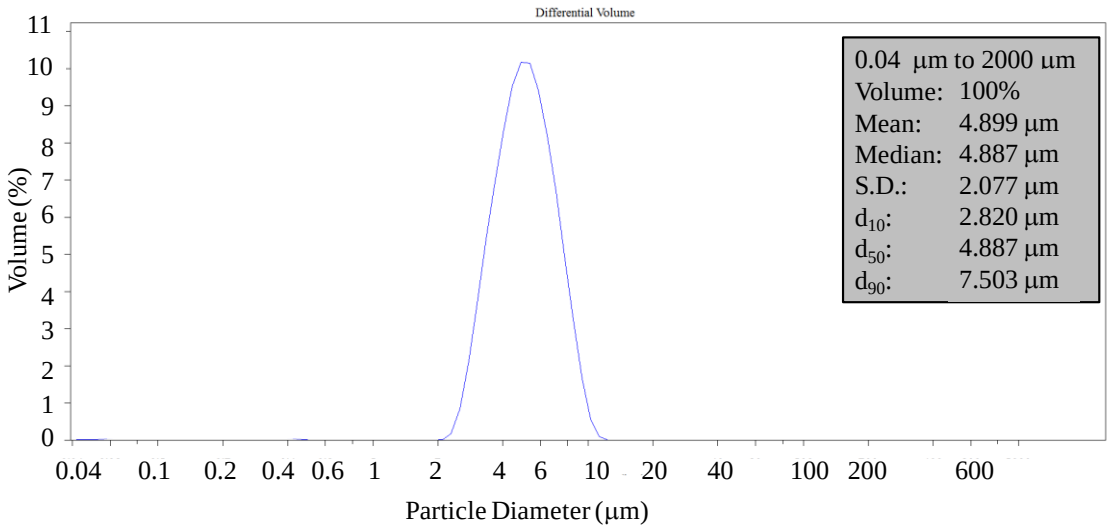

Figure 1. Particle Size Distribution of PCS Micronal® DS 5007 X.

The evolution over time for PCS28 results is plotted in Figure 2. This graph illustrates that at the beginning of the experiment there was a bimodal distribution showing two peaks, one corresponding to a fraction of particles with smaller size and the other one corresponding to bigger particles. After 10 minutes (1 minute per each cycle) inside the circuit, the distribution shows one peak. Therefore, an agglomeration particle process was obtained over time for this sample.

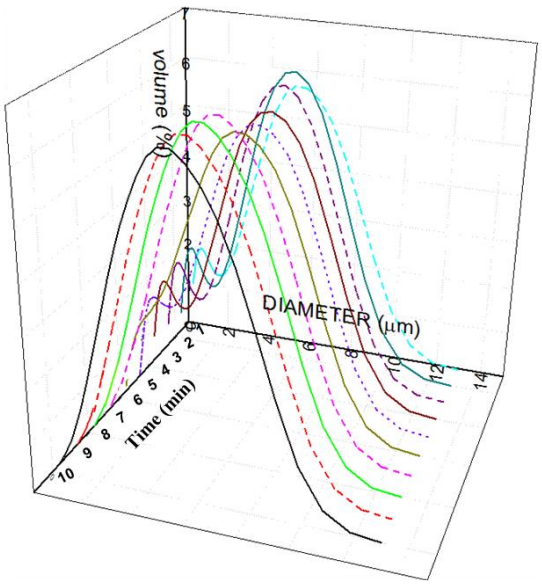

Figure 2. Particle Size Distribution progress of the PCS28 slurry in front of time.

3.1.2. Scanning Electron Microscopy (SEM)

SEM images of the two samples are shown in Figure 3. It was done a drying process at room temperature to better observe the size of the PCS microcapsules, followed by a compression of the sample to crash the microcapsules. Particle sizes (left) and wall thicknesses (right) are detailed in this figure. For both samples, Micronal® DS 5007 X and PCS28, the particle size is variable. Note that the samples under study show approximately the same shell thickness, which is around 0.5 µm. Furthermore, the main results for microcapsules size and wall shell thickness are listed in Table 2.

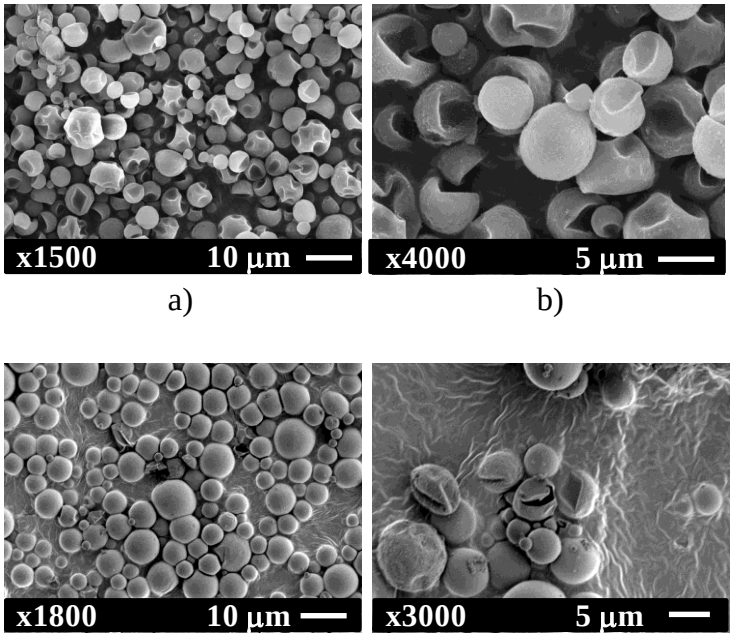

Figure 3. SEM images. (a) PCS Micronal® DS 5007 X x 1,500, (b) PCS Micronal® DS 5007 X x 4,000; and (c) PCS28 x 1,600, (d) PCS28 x 3,000

Table 2. SEM results from microcapsules under study

	Micronal® DS 5007 X	PCS28
Size (µm)	4.0 - 8.0	2.1 - 10.2
Size wall thickness shell (µm)	0.5	0.5

3.2. Atomic Force Microscopy

3.2.1. Micronal®DS 5007 X

The typical loading curve for Micronal® DS 5007 X at 23 ºC is shown in Figure 4. The deflection error *vs*. Z is represented, where the deflection error is proportional to the applied force, and Z is the penetration of the tip inside the sample. At the beginning of the experiment there is no force applied (a). Subsequently, in this case, applying 11 µN of load (transition (b) to (c)) the microcapsule breaks. The tip penetrated around 0.6 µm,

allowing to observe the created hole in the position where the AFM probe has punctured. Finally, the unloading curve shows the retracting of the tip (d).

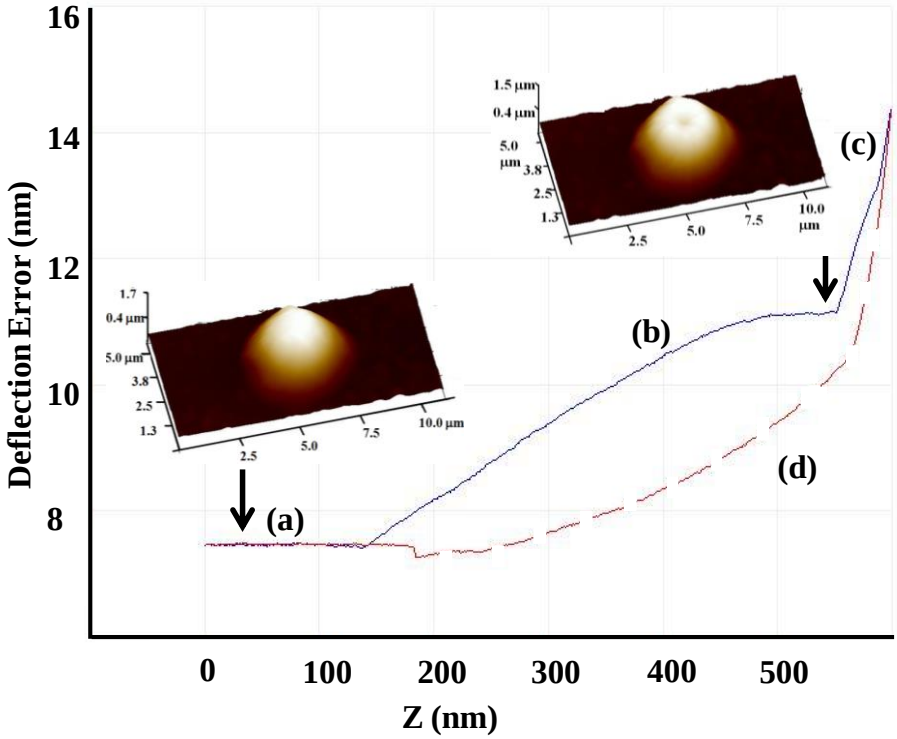

Figure 4. Mechanical testing of the elastic-plastic region by AFM of a Micronal® DS 5007 X microcapsule at 23 ºC, (a) no contact, continuous line; (b) plastic penetration; (c) deformation of the sample; and (d) retraction of the AFM probe, discontinuous line.

The same procedure of puncturing the sample was done at 45 ºC, as Figure 5 shows. In this case, the indentation breakthrough occurs at 1.8 µN, because the higher the temperature, the softer the polymer.

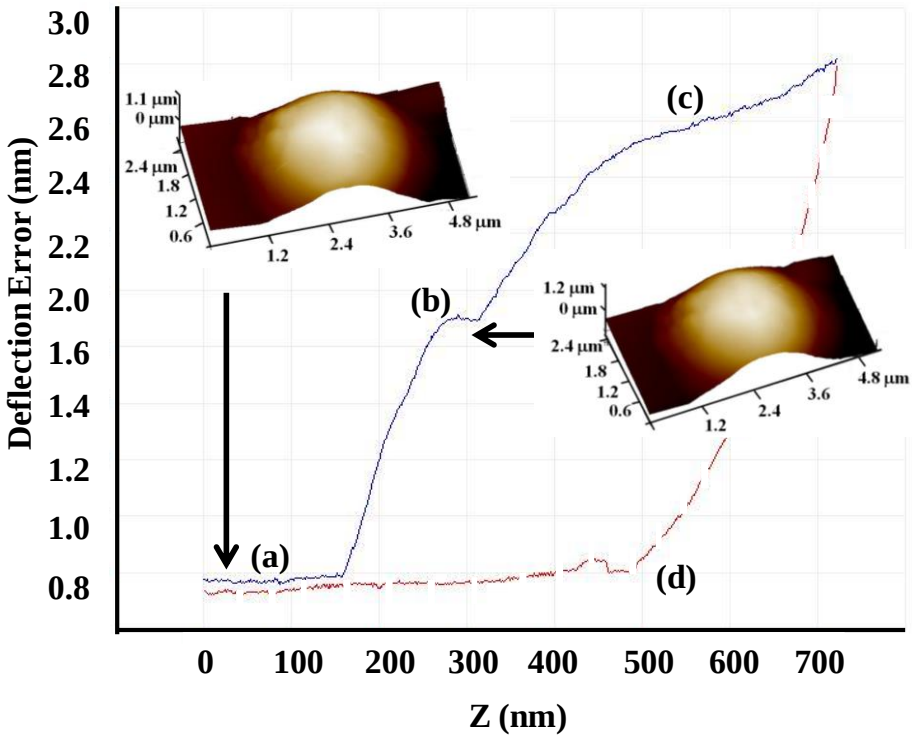

195

196 Figure 5. Mechanical testing of the elastic-plastic region by AFM of Micronal® DS 5007
197 X microcapsule at 45 ºC; (a) no contact, continuous line; (b) plastic penetration; (c)
198 deformation of the sample; and (d) retraction of the AFM probe, discontinuous line.

199

200 It is important to note that when a microcapsule is heated up, the topographic
201 section may change. This effect can be observed in Figure 6 where it can be seen the 3D
202 view (Figure 6, 1a and 2a) and the profile of the white line of a microsphere (Figure 6,
203 1b and 2b) at different temperatures, 23 ºC and 45 ºC.

204

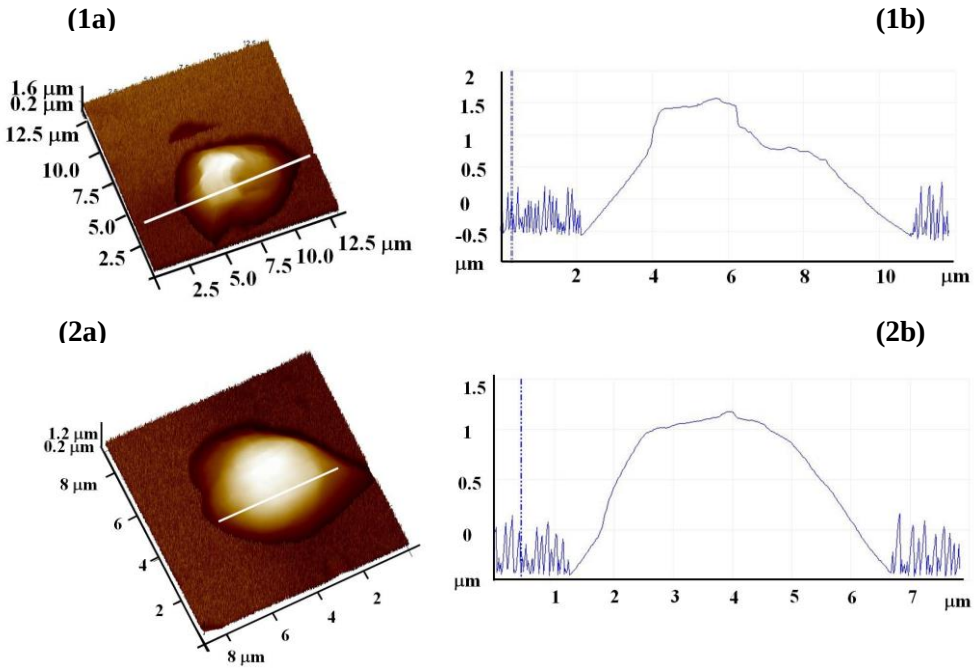

Figure 6. Micronal® DS 5007 X sample (1a) 3D view at 23 ºC; (2a) 3D view at 45 ºC; (1b) topographic image at 23 ºC; (2b) topographic image at 45 ºC.

Furthermore, a mechanical map at 23 ºC and 0.5 KHz per second in Giro-Paloma *et al.* study was evaluated [17] obtaining a great dispersion of values, being between 10 to 20 nm of deformation. Besides, applying a vertical force of 500 nN on the top of the microcapsule, *E* values show a great dispersion being the mean value about 200 MPa.

E mapping diagram for Micronal® DS 5007 X was measured also at 45 ºC, and the region studied is shown in Figure 7(a). The total pixels amount of the area selected is represented the Y axis. In this case, from the deformation histogram, deformation varies around 20 nm (b), and the calculated results of the *E* histogram applying 500 nN were around 50 MPa (c), four times lower than the experiments at 23 ºC due to the softening of the particle shell as well as the liquid state of PCM. The mechanical properties hastily reduced when the temperature increase and it is close to the glass transition, for Micronal® samples.

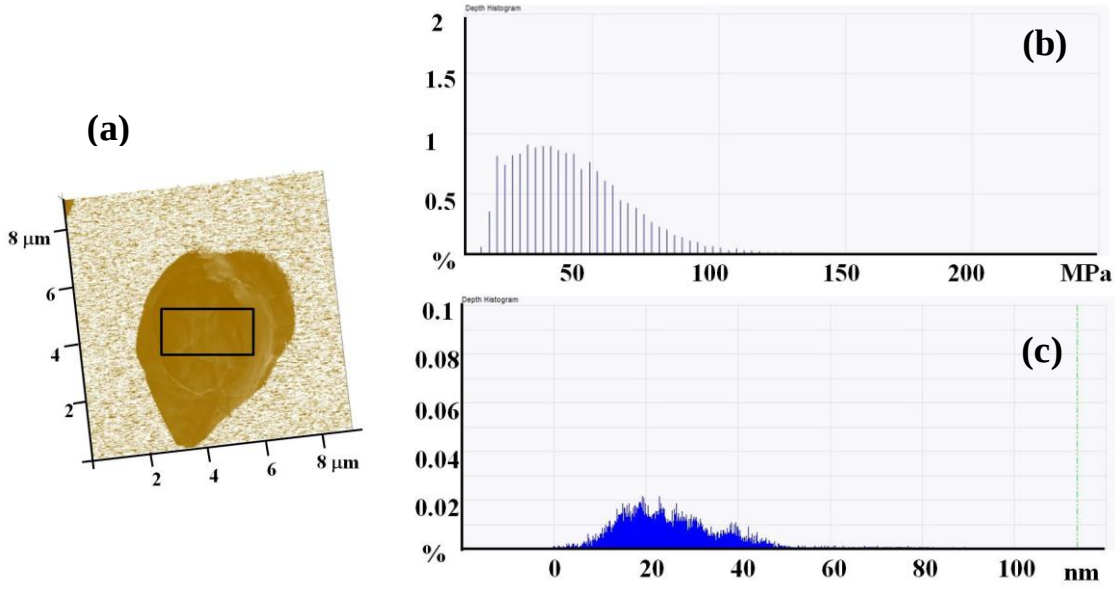

Figure 7. Effective Young's modulus mapping of Micronal® DS 5007 X at 45 ºC; (a) 3D view; (b) Deformation histogram (nm); (c) *E* histogram (GPa).

3.2.2. PCS28

The experimental procedure at 23 ºC was also performed for PCS28. The mechanical testing loading AFM curve of deflection error *vs.* Z is shown in Figure 8. Then, applying 2.5 µN the sample breaks and a permanent indenter print is observed in the sample (Figure 8b).

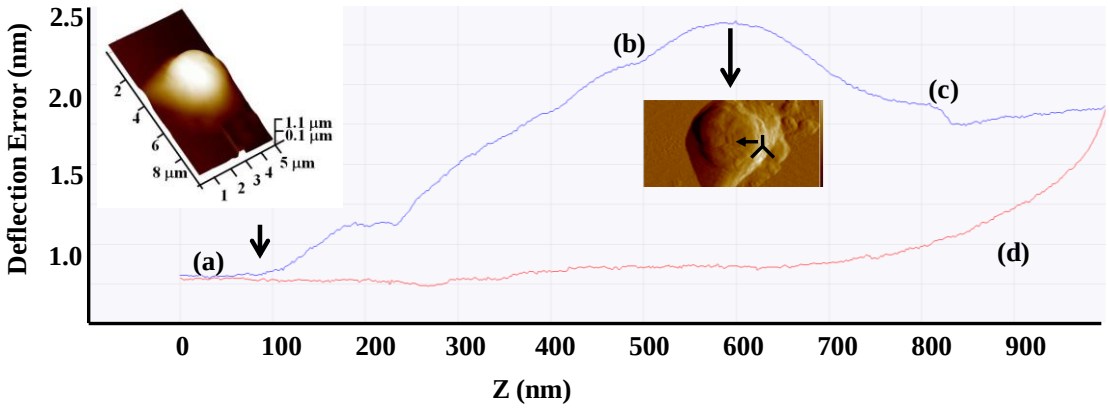

Figure 8. Mechanical testing of the elastic-plastic region by AFM of a microcapsule of PCS28 at 23 ºC; (a) no contact, continuous line; (b) plastic penetration; (c) deformation of the sample; and (d) retraction of the AFM probe (red line).

Afterwards, an identical process of penetrating the microsphere with a tip was done at 45 ºC, as it is seen in Figure 9. This microsphere breaks at lower force (0.9 μN) compared with the experiment performed at 23 ºC. The particle was punctured, and the inner phase change wax material spread on the mica surface, as (b) confirms.

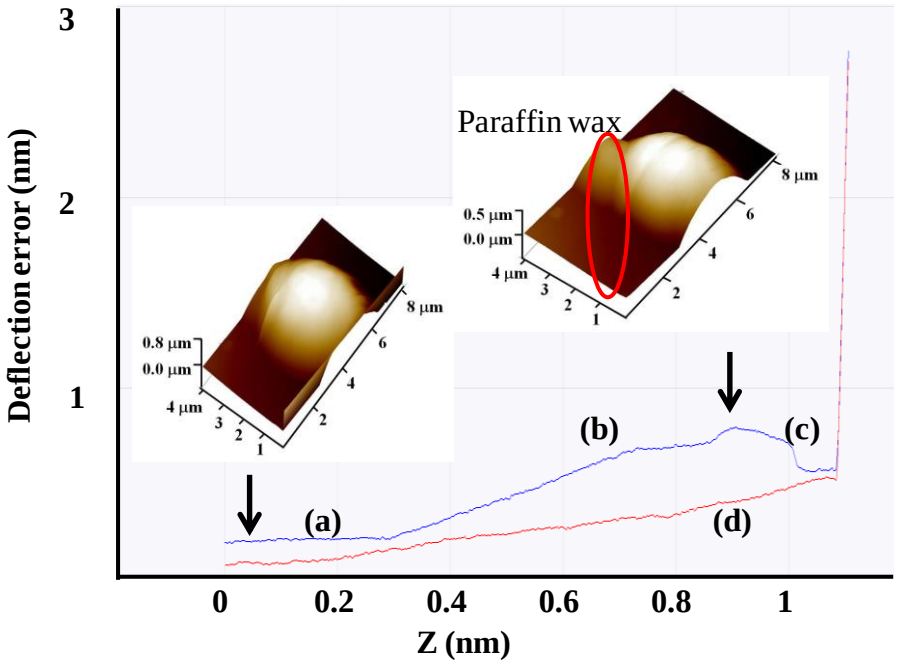

Figure 9. Mechanical testing of the elastic-plastic region by AFM of a microcapsule of PCS28 at 45 ºC; (a) no contact, continuous line; (b) plastic penetration; (c) deformation of the sample; and (d) retraction of the AFM probe (red line).

When heating a microcapsule of PCS28 from 23 to 45 ºC, the topographic section of 10 x 10 μm corresponding to the white line in the image changes. This mentioned change is shown in Figure 10.

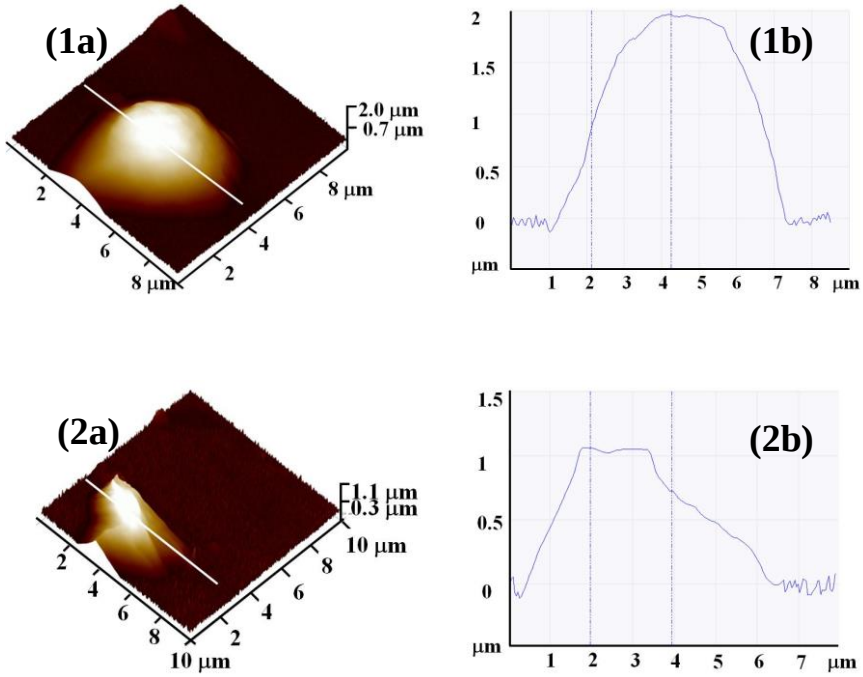

Figure 10. PCS28 sample at (1) 23 ºC and, (2) 45 ºC; (a) 3D view, and (b) topographic image.

The 3D view *E* map (a), the deformation histogram (b), and *E* histogram (c) of PCS28 at 23 ºC are presented in Figure 11. The obtained results were 70 nm for the mean deformation and 43 MPa applying a vertical force of 500 nN. These results show that PCS28 particles are clearly softer than the Micronal® DS 5007 X resulting in more deformable particles.

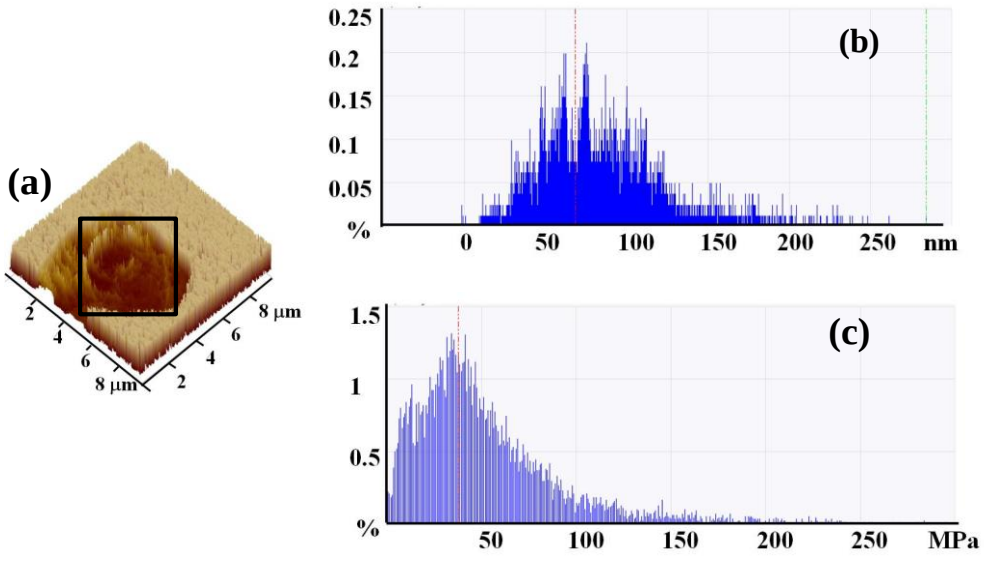

Figure 11. Effective Young's modulus mapping of PCS28 at 23 ºC; (a) 3D view; (b) Deformation histogram; (c) *E* histogram.

Additionally, *E* mapping at 45 ºC for PCS28 is shown in Figure 12. As it happens with Micronal® DS 5007 X, the obtained values at 45 ºC are even lower compared to those achieved at 23 ºC. The deformation values were between 70 and 300 nm, and the mean *E* result was 30 MPa using 500 nN of load.

The mechanical properties when increasing the temperature for PCS28 sample also decrease because of the MF polymeric shell, since is a thermoset resin has the tendency to have more fragile and pressure-sensitive walls compared with acrylic one, it is susceptible to break and degrade more easily. Therefore, results demonstrate that acrylic polymeric shell for MPCM for PCS is a better option compared to MF. Nevertheless, the measurements were not performed in pumping conditions.

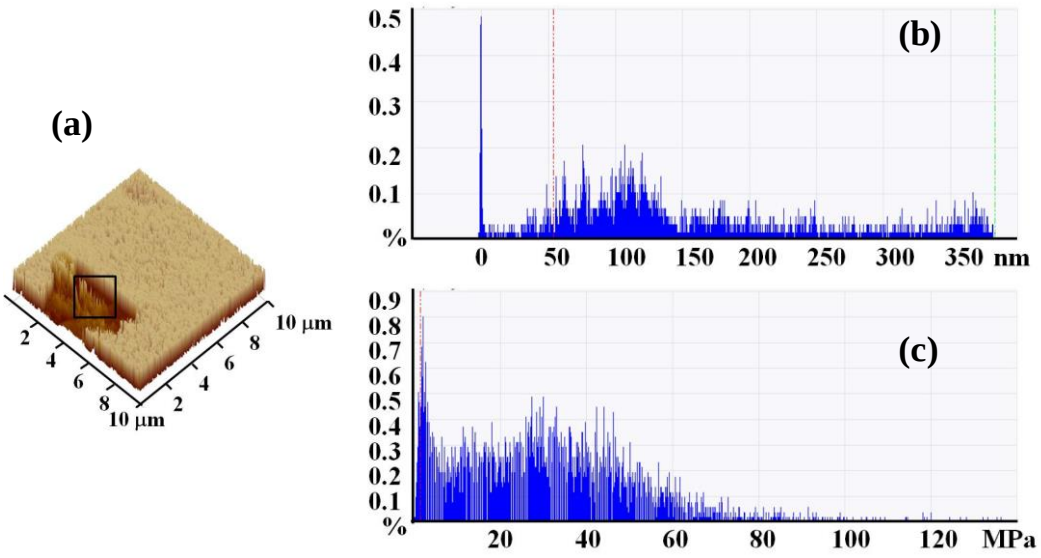

Figure 12. Effective Young's modulus mapping of PCS28 at 45 ºC; (a) 3D view; (b) Deformation histogram; (c) E histogram.

Table 3 summarizes the obtained results by means AFM technique.

277

278 Table 3. Summary of the main results.

	Micronal® DS 5007 X		PCS 28	
	23 ºC	**45 ºC**	**23 ºC**	**45 ºC**
Needed force to break the MPCM (μN)	11.0	1.8	2.5	0.9
Deformation (nm)	10-20	20	70	70-300
Mean Effective Young's modulus (*E*) value applying 500 nN (MPa)	200	50	43	30

279

280 ## 4. Conclusions

281 Two different samples of PCS containing microcapsules with different polymeric
282 shell and paraffin wax as PCM were compared in this paper. Micronal® DS 5007 X
283 presents a bigger particle size than PCS28 sample. Furthermore, PCS28 sample shows
284 an agglomeration over time. Additionally, the samples under study have similar wall
285 shell thickness, around 0.5 μm. From the mechanical viewpoint, AFM technique
286 demonstrates that it is very important to take into consideration the assay temperature,
287 because the mechanical properties decrease abruptly when the temperature increases.
288 The mechanical properties are reduced abruptly when the temperature is close to the
289 glass transition for Micronal® samples. In case of PCS28 its reduction is due to nature
290 of prepared microcapsule wall using in situ polymerisation and melamine-formaldehyde
291 as shell material, which tend to have more brittle and pressure-sensitive walls, and were
292 prone to cracking. Also, it is essential to consider the change in shape of the
293 microcapsules with an increment of temperature for the studied samples. The higher the
294 temperature, the lower the mechanical properties and this fact also is influenced by the
295 liquid state of the paraffin wax. The needed force to break Micronal® DS 5007 X
296 microcapsules decrease one order of magnitude when changing the temperature from 23
297 ºC to 45 ºC. Comparing Micronal® DS 5007 X with PCS28, the properties obtained
298 from the mechanical performance are higher. In summary, from the mechanical point of
299 view, an acrylate group to be used as a shell of microcapsules is better than a melamine-
300 formaldehyde resin taking into account that both samples have the same thickness shell
301 as SEM results elucidate. But, using MF as a MPCM shell, walls can be improved
302 getting more durable, and this is also influenced by the fabrication process: laboratory

or industrial. Hence, results show that acrylic polymeric shell is a better choice in comparison to MF, where it is difficult to change its wall brittle nature to desire more elastic. However, these measurements were performed using static samples. More experiments must be performed under pumping conditions.

Acknowledgments

The work is partially funded by the Spanish government (ENE2011-28269-C03-02 and ENE2011-22722). The authors would like to thank the Catalan Government for the quality accreditation given to their research group GREA (2014 SGR 123) and research group DIOPMA (2014 SGR 1543). The research leading to these results has received funding from the European Union's Seventh Framework Programme (FP7/2007-2013) under grant agreement nº PIRSES-GA-2013-610692 (INNOSTORAGE).

References

[1] Mehling H, Cabeza LF. Heat and cold storage with PCM. Springer-Verlag. ISBN-13: 9783540685562, 2008.

[2] Zhou D, Zhao CY, Tian Y. Review on thermal energy storage with phase change materials (PCMs) in building applications. Appl Energ 2012;92:593-605.

[3] Kuznik F, David D, Johannes K, Roux JJ. A review on phase change materials integrated in building walls. Renew Sust Energ Rev 2011;15:379-91.

[4] Sharma A, Tyagi VV, Chen CR, Buddhi D. Review on thermal energy storage with phase change materials and applications. Renew Sust Energ Rev 2009;13:318-45.

[5] Agyenim F, Hewitt N, Eames P, Smyth M. A review of materials, heat transfer and phase change problem formulation for latent heat thermal energy storage systems (LHTESS). Renew Sust Energ Rev 2010;14:615-28.

[6] Schossig P, Henning HM, Gschwander S, Haussmann T. Micro-encapsulated phase change materials integrated into construction materials. Sol Energ Mat Sol C 2005;89:297-306.

[7] Tyagi VV, Buddhi D. PCM thermal storage in buildings: A state of the art. Renew Sust Energ Rev 2007;11:1146-66.

[8] Borreguero AM, Carmona M, Sánchez ML, Valverde JL, Rodríguez JF. Improvement of the thermal behavior of gypsum blocks by the incorporation of microcapsules containing PCMs obtained by suspension polymerization with an optimal core/coating mass ratio. Appl Therm Eng 2010;30:1164-9.

[9] Ling TC, Poon CS. Use of phase change materials for thermal energy storage in concrete: An overview. Constr Build Mater 2013;46:55-62.

[10] Vectstaudza J, Locs J, Bajāre D, Barreneche C, Fernández AI. Characterization of Wood/PCM Composites for Building Applications. The 2nd International Energy Stoarge Conference. Sustainable Energy Storage in buildings, 2013.

[11] Bayés-García L, Ventolà L, Cordobilla R. Phase change materials (PCM) microcapsules with different shell compositions: preparation, characterization and thermal stability. Sol Energ Mater Sol C 2010;94:12535-40.

[12] Giro-Paloma J, Oncins G, Barreneche C, Martínez M, Fernández AI, Cabeza LF. Physico-chemical and mechanical properties of microencapsulated phase change material. Appl Energ 2013;109:441-8.

[13] Zhao CY, Zhang GH. Review on microencapsulated phase change materials (MEPCMs): Fabrication, characterization and applications. Renew Sust Energ Rev 2011;15:3813-32.

[14] Salunkhe PB, Shembekar PS. A review on effect of phase change material encapsulation on the thermal performance of a system. Renew Sust Energ Rev 2012;16:5603-16.

[15] Tyagi VV, Kaushik SC, Tyagi SK, Akiyama T. Development of phase change materials based microencapsulated technology for buildings: a review. Renew Sust Energ Rev 2011;15:1373-91.

[16] Castellon C, Medrano M, Roca J, Cabeza LF, Navarro ME, Fernandez AI. Effect of microencapsulated phase change material in sandwich panels. Renew Energ 2010;35(10):2370-74.

[17] Giro-Paloma J, Barreneche C, Delgado M, Martínez M, Fernández AI, Cabeza LF. Physicochemical and thermal study of a MPCM of PMMA shell and paraffin wax as a core. Energy Procedia 2014;48:347-54.

[18] Delgado M, Lázaro A, Mazo J, Marín JM, Zalba B. Experimental analysis of a microencapsulated PCM slurry as thermal system and as heat transfer fluid in laminar flow. Appl Therm Eng 2012;36(1):370-7.

[19] Lu W, Tassou SA. Experimental study of the thermal characteristics of phase change slurries for active cooling. Appl Energ 2012;91(1):366-74.

[20] Zhang S, Niu J. Experimental investigation of effects of super-cooling on microencapsulated phase-change material (MPCM) slurry thermal storage capacities. Sol Energ. Mat Sol C 2010;94(6):1038-48.

[21] Youssef Z, Delahaye A, Huang L, Trinquet F, Fournaison L, Pollerberg C, Doetsch C. State of the art on phase change material slurries. Energ Convers Manage 2013;65:120-32.

[22] Delgado M, Lázaro A, Mazo J, Zalba B. Review on phase change material emulsions and microencapsulated phase change material slurries: materials heat transfer studies and applications. Renew Sust Energ Rev 2012;16(1):253-73.

[23] Castellón C, Martorell I, Cabeza LF, Fernández AI, Manich AM. Compatibility of plastic with phase change materials (PCM). Int J Energ Res 2010;35:765-71.

[24] Zhang GH, Zhao CY. Thermal and rheological properties of microencapsulated phase change materials. Renew Energ 2011;36:2959-66.

[25] Šumiga B. Ph.D Thesis, University of Ljubljana, 2013

[26] Su JF, Wang LX, Ren L. Preparation and characterization of double-MF shell microPCMs used in building materials. J Appl Polym Sci 2005;97(5):1755-62.

[27] Giro-Paloma J, Barreneche C, Martínez M, Sumiga B, Cabeza LF, Fernández AI. Comparison of phase change slurries: Physicochemical and thermal properties. Energy 2015;87:223-227.

[28] VanLandingham MR, Villarrubia JS, Meyers GF. Nanoindentation of polymers: overview. Polymer preprints 2000;41(2):1412.

[29] Clifford CA, Seah MP. Nanoindentation measurement of Effective Young's modulus for compliant layers on stiffer substrates including the effect of Poisson's ratios. Nanotechnology 2009;20:1-8.

[30] Giro-Paloma J, Roa JJ, Díez-Pascual AM, Rayón E, Flores A, Martínez M, Chimenos JM, Fernández AI. Depth-sensing indentation applied to polymers: A comparison between standard methods of analysis in relation to the nature of the materials. Eur Polym J 2013;49:4047-53.